JOURNAL OF MATERIALS SCIENCE 31 (1996) 3223–3229

Control of calcium hexaluminate grain morphology in *in-situ* toughened ceramic composites

L. AN, H. M. CHAN
Department of Materials Science & Engineering, Lehigh University, Bethlehem, PA 18015, USA

K. K. SONI
Enrico Fermi Institute, University of Chicago, Chicago, IL 60637-1433, USA

The influence of processing conditions on the morphology of calcium hexaluminate (CA_6) grains in Al_2O_3: 30 vol % $CaO{\cdot}6Al_2O_3$ (CA_6) ceramic composites was investigated. Specimens were prepared by *in-situ* reaction sintering using precursor powders of alumina, and either calcium carbonate or calcium oxide. In some samples, 1 vol % anorthite glass was added as a sintering aid. X-ray diffraction was used to study the phase development in the as-calcined and sintered states. The resultant microstructures were characterized using both scanning electron microscopy (SEM), and imaging secondary ion mass spectrometry (SIMS). It was found that the CA_6 grains developed a platelike morphology when $CaCO_3$ was used as the starting calcium-rich powder. In contrast, samples prepared using CaO resulted in equiaxed CA_6 grains. This result was observed to be independent of the anorthite glass addition. The findings are rationalized in terms of distinct CA_6 reaction mechanisms, resulting from differences in the reactivity of the powders during the early stages of calcining.

1. Introduction

Recently, there has been renewed interest in the processing of ceramics whose microstructures exhibit platelike grain morphologies. This has arisen in great part due to the growing awareness that elongated grains can act as bridging sites in the wake of a crack, hence resulting in improved mechanical behaviour. In addition, potential health hazards associated with the fabrication of whisker reinforced composites are completely circumvented. A notable example of this type of "*in-situ* toughened" material is self-reinforced Si_3N_4 [1–5]. In this case, the presence of highly elongated β-Si_3N_4 grains results in significant improvements in the fracture toughness and Weibull modulus compared to fine-grained Si_3N_4 materials [1, 4].

Clearly, the potential exists for exploiting the concept of *in-situ* reinforcement in oxide ceramics. Possible advantages over the Si_3N_4 based materials would include greater ease of processing due both to lower sintering temperatures, and the ability to utilize air versus controlled atmosphere furnaces. Furthermore, such materials would exhibit improved oxidation resistance at elevated temperatures. Several studies have shown that in Al_2O_3/TZP materials, the incorporation of platelet hexaluminate grains can lead to significant mechanical behaviour enhancement [6–8]. In such transformation toughened materials, however, the role of the platelet phase is considerably more complex, since it may also act to limit autocatalytic transformation, and/or modify the degree of transformation plasticity. Most recently, Chen and Chen [9] studied the mechanical behaviour of a series of *in-situ* alumina/aluminate ($LaAl_{11}O_{18}$, $LaMgAl_{11}O_{19}$, $SrAl_{12}O_{19}$ and $Mg_2NaAl_{15}O_{25}$) composites. Although improved toughness due to bridging by the aluminate grains was observed, the maximum toughness was intrinsically limited by the low strength of these layered compounds.

A closely analogous *in-situ* reinforced composite system which to date has received little attention is that of Al_2O_3–$CaAl_{12}O_{19}$. The Al_2O_3–CaO systems contains a number of stable intermediate compounds (C_3A, $C_{12}A_7$, CA, CA_2, and CA_6)[1], of which calcium hexaluminate (CA_6) is the most alumina rich [10]. CA_6 possesses the magnetoplumbite structure (space-group $P6_3/mmc$) [11], and is an important component of high temperature cements and refractories. Both the mechanical [12, 13] and thermal expansion [14] properties of CA_6 render it a promising *in-situ* reinforcement phase. Of particular interest from our standpoint, however, was that preliminary studies revealed that the morphology of the CA_6 grains could be readily changed (from equiaxed to platelet) by modifying the processing conditions. Although

[1] Cement nomenclature: C is CaO and A is Al_2O_3.

0022–2461

these differences in morphology have been reported by other workers [15], there has been no detailed study of this phenomenon. The present work describes the results of a study aimed at understanding the development of platelike CA_6 grain morphologies in reaction sintered alumina–calcium hexaluminate composites. The mechanical behaviour of these materials will be discussed separately.

2. Experimental procedure

Composites of alumina: 30 vol % calcium hexaluminate were prepared by *in-situ* reaction sintering. High purity submicron alumina (Sumitomo, AKP-HP), calcium carbonate (Johnson Matthey, 10996), and calcium oxide were used as starting powders. The calcium oxide was obtained by calcining the $CaCO_3$ at 1000 °C for 2 h. Complete decomposition of the $CaCO_3$ powder was confirmed by weight loss measurements. Samples of the $CaCO_3$ and CaO powders were sent to a commercial laboratory for impurity analysis by ICP (inductively coupled plasma). It was found that both the types and levels of cation impurity were very similar in both cases. Specifically, the MgO content was found to be < 10 ppm for both powder batches.

Two different starting powder mixtures were utilized: a) alumina and calcium carbonate, and b) alumina and calcium oxide. The ratio of alumina to calcium carbonate (or calcium oxide) required to form 30 vol % of CA_6 phase was calculated from the equilibrium phase diagram [10]. One vol % anorthite glass ($CaO \cdot Al_2O_3 \cdot 2SiO_2$) was added into both powder mixtures as a sintering additive. In addition, a third powder mixture of alumina and calcium carbonate was prepared without the glass phase. All of the powder mixtures were ball milled in methanol for 24 h, using zirconia ball-grinding media. The homogeneous slurry was then dried whilst being continuously stirred on a stirrer/hot-plate. The dried powder was die-pressed at 50 MPa, and then isostatically pressed at 350 MPa. The green pellets were calcined at either 1200 or 1400 °C for 12 h, followed by pressureless sintering for 2 h at 1650 °C. A summary of the starting powder compositions and heat-treatment conditions is given in Table I. The densities of the composites were measured using the Archimedes method with water as the immersion medium.

The phases present in the as-calcined and sintered states were determined using powder X-ray diffraction (Cu K-α radiation). Fortunately, the different calcium aluminate phases are readily distinguishable [15], since there is little overlap between their major diffraction peaks. Samples for microstructural characterization were polished to 1 μm finish, and thermally etched at 1400 °C for 1 h. The microstructure was observed using a scanning electron microscope (SEM) equipped with an energy-dispersive spectrometer (EDS). For selected samples, elemental mapping was performed by imaging secondary ion mass spectrometry (SIMS) on polished, unetched surfaces. These samples were sputter-coated with a thin layer of gold in order to reduce charging effects during the analyses. SIMS analysis was carried out using a scanning ion microprobe developed at the University of Chicago [16, 17]. In this instrument, a focused beam (diameter ~ 50 nm) of gallium ions is scanned over the specimen surface to erode atoms by a sputtering process. The emitted secondary ions are mass resolved in a double focusing magnetic sector mass spectrometer. In addition to chemical mapping, topographic images can be obtained by collecting the total ion-induced secondary ion (ISI) signal without mass discrimination. In the present study, the accelerating voltage of the gallium ions was 40 keV, and the beam current was ~ 40 pA.

3. Results

The results of the X-ray diffraction study on the phases present in the as-calcined and sintered samples are summarized in Fig. 1, which is a "flowchart" depicting the sequence of microstructural changes for the different processing conditions and starting powder compositions. Note that the different calcining temperatures (1200 and 1400 °C) are represented by dashed and solid lines respectively; and the starting powder compositions (1, 2 and 3) are distinguished by flowlines of different thickness. By comparing the phase composition/morphology developed at different stages of heat-treatment for the three starting powder compositions, we can make the following interesting deductions.

TABLE I Starting powder compositions, processing conditions and final microstructure

Composites	Starting powders	Heat-treatment conditions*	Final density (% TD)	Phases present and grain morphology	
				Al_2O_3	$CaO \cdot 6Al_2O_3$
A: $30CA_6$ (1)	Al_2O_3, $CaCO_3$,	Calcined: 1200 °C for 12 h	97.0	Equiaxed	Elongated
	Anorthite glass	Calcined: 1400 °C for 12 h	97.3	Equiaxed	Elongated
A: $30CA_6$ (2)	Al_2O_3, $CaCO_3$	Calcined: 1200 °C for 12 h	98.1	Equiaxed	Elongated
		Calcined: 1400 °C for 12 h	98.2	Equiaxed	Elongated
A: $30CA_6$ (3)	Al_2O_3, CaO,	Calcined: 1200 °C for 12 h	98.4	Equiaxed	Equiaxed
	Anorthite glass	Calcined: 1400 °C for 12 h	98.4	Equiaxed	Equiaxed

* All samples were sintered at 1650 °C for 2 h.

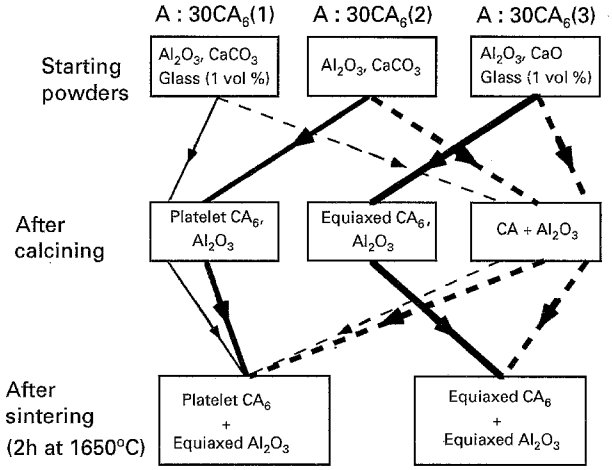

Figure 1 Flowchart showing the phase development in both as-calcined and sintered states. The different calcining temperatures (1200 °C and 1400 °C for 12 h) are represented by dashed and solid lines respectively. The starting powder compositions are differentiated by using lines of different thickness.

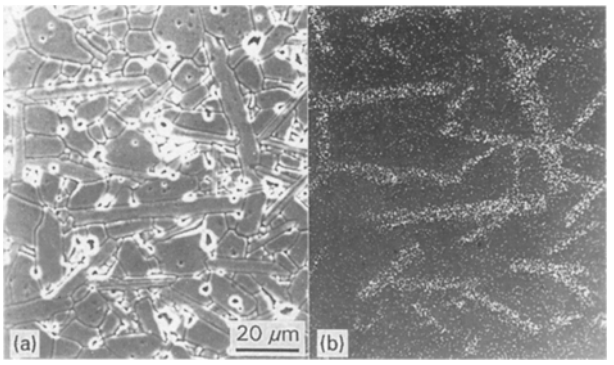

Figure 2 SEM micrographs of A: 30CA_6 (1) showing elongated plate-like morphology of CA_6 grains: (a) Secondary electron image, (b) corresponding Ca X-ray map.

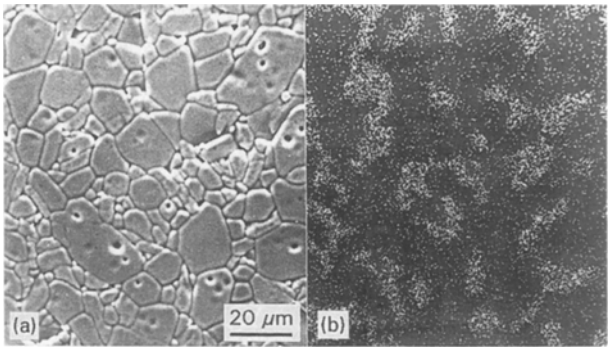

Figure 3 SEM micrographs of A: 30CA_6 (3) showing equiaxed morphology of CA_6 grains: (a) Secondary electron image, (b) corresponding Ca X-ray map.

If we first consider the as-calcined samples, it can be seen that the lower calcining temperature (1200 °C) favours the development of the monocalcium aluminate – $CaAl_2O_4$ (CA), whereas calcining at 1400 °C results in the formation of CA_6. Thus the *composition* of the intermediate calcium aluminate phase (CA vs. CA_6) appears to be controlled solely by the calcining temperature. Interestingly, however, the *morphology* of the CA_6 phase is different depending on the precursor powders. This same difference in morphology is retained in the final sintered microstructures (see Figs 2 and 3). Namely, in the case where CaO was used as the precursor calcium containing powder, equiaxed CA_6 grains were obtained. In contrast, the use of $CaCO_3$ (both with and without anorthite glass) resulted in elongated plate-like CA_6 grains. Intriguingly, this observation applied even for samples calcined at 1200 °C, where all three starting powder mixtures formed CA after calcining.

A montage of SIMS maps obtained from the same area of specimen A: 30CA_6 (1) is shown in Fig. 4. From the ISI map (Fig. 4a), it is possible to discern topographical contrast due to the presence of the CA_6 platelets and glass phase. The morphology of the CA_6 platelets is clearly revealed in the Ca SIMS map, whereas the alumina matrix dominates in the Al map. The glass phase is readily identifiable in the Si map. The corresponding compositional maps for specimen A: 30CA_6 (3) is given in Fig. 5. The equiaxed morphology of the CA_6 grains in this specimen is confirmed by the Ca and Al maps. With regard to the faint background in the Si maps for both specimens, this is the result of overlap between the $^{28}Si^+$ and $^{28}AlH^+$ signals. Fortunately, this does not complicate our interpretation of the glass distribution, because the $^{28}AlH^+$ signal is very weak in comparison to the Si signal from glass. Interestingly, a comparison of Figs 4d and 5d [2]reveals that the distribution of Mg in the two samples is different. Specifically, in the platelet composite, the Mg concentration is higher in the CA_6 phase than in the alumina matrix, whereas in the equiaxed composite, the situation is reversed.

4. Discussion

4.1. General

This observed sensitivity of the CA_6 morphology to the Ca-containing precursor powder has not been reported previously. The result is particularly surprising, given that: a) the CaO was obtained by calcination of $CaCO_3$ derived from the same source as that used for the other samples, and b) chemical analysis did not reveal any significant differences in the trace impurities in the starting powders. Furthermore, although it is well known that the development of plate-like grains is often linked to the presence of glassy grain boundary phases, this cannot completely account for the results of the present study, because sample A: 30CA_6 (3) developed equiaxed CA_6 grains, despite the presence of 1 vol % anorthite glass.

Neither does the *sequence* of calcium aluminate phase formation seem to be an important factor in determining the CA_6 grain structure. For example, comparison of samples A: 30CA_6 (1) and A: 30CA_6 (3) for the 1200 °C calcining temperature showed that

[2] No quantitative analysis of Mg was attempted. However, given the extremely high sensitivity of the SIMS technique towards Mg (particularly in oxide matrices), the reported Mg maps are not inconsistent with the overall low Mg content (< 10 ppm).

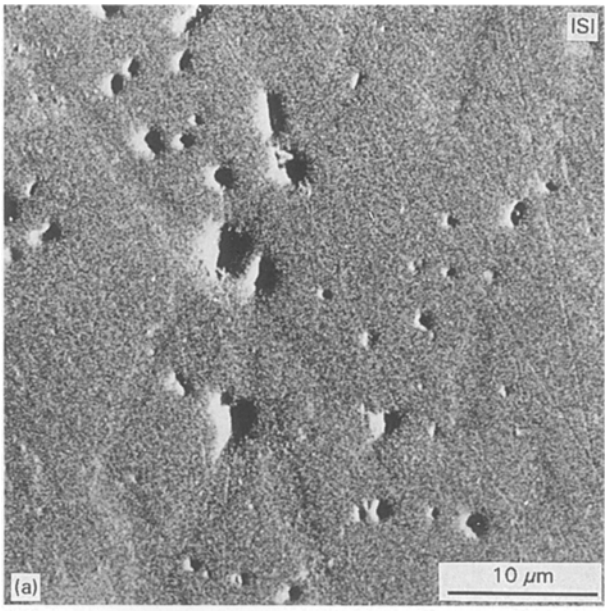

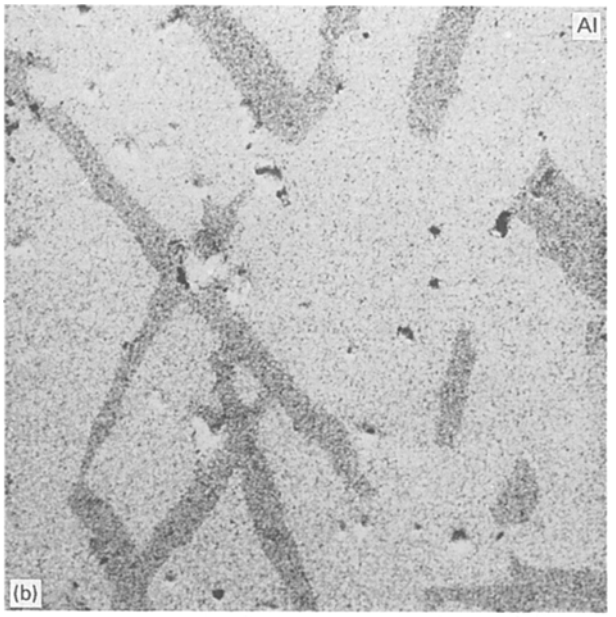

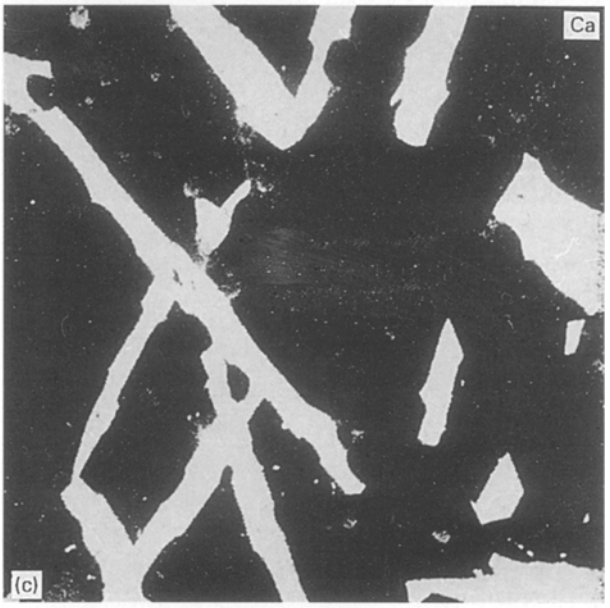

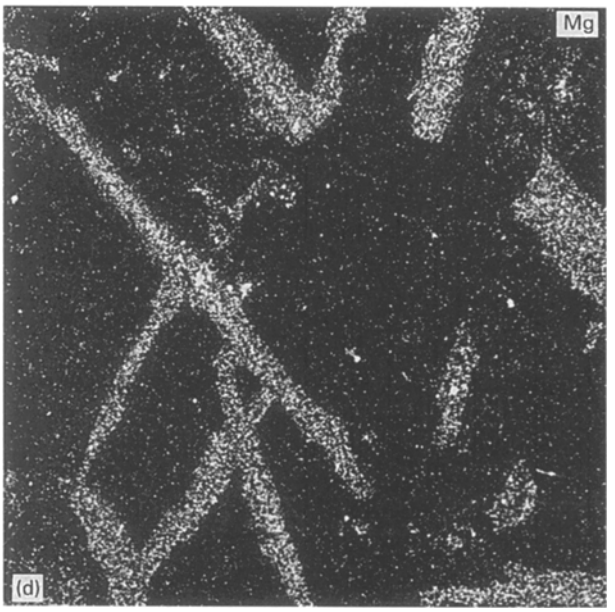

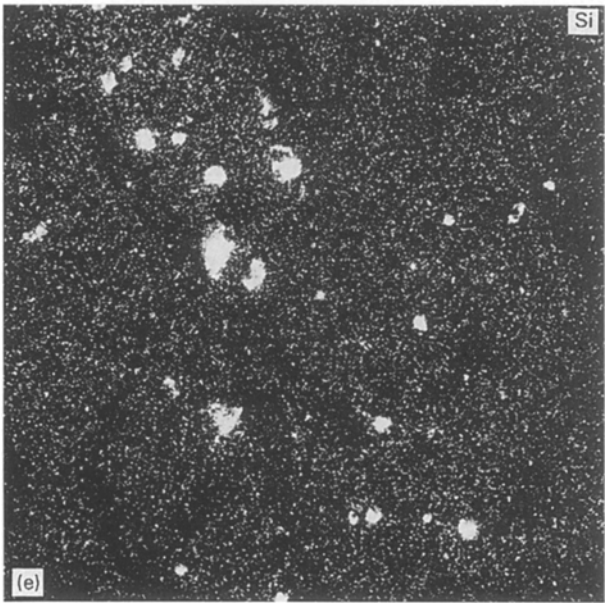

Figure 4 SIMS images obtained from specimen A: $30CA_6$ (1): (a) Total ion-induced secondary ion (ISI) image showing topographic contrast. Chemical distribution maps: (b) Al^+, (c) Ca^+, (d) Mg^+, and (e) Si^+. Images are shown using a logarithmic gray scale to aid contrast interpretation. Note that the Mg concentration is higher in the plate-like CA_6 grains than in the alumina matrix.

both samples consisted predominately of Al_2O_3 and CA after calcination, and yet on sintering, developed different CA_6 morphologies.

4.2. Proposed model

The question remains, therefore, what is causing the difference in the microstructures of the Al_2O_3: CA_6 composites? Although it is difficult to provide a definitive explanation, we can put forward the following model. During the early stages of calcining, monocalcium aluminate is formed by solid state reaction in the powder compact. This is evident both from the present study, and that of Mendoza *et al.* [15], who reported that the optimum calcining temperature for CA

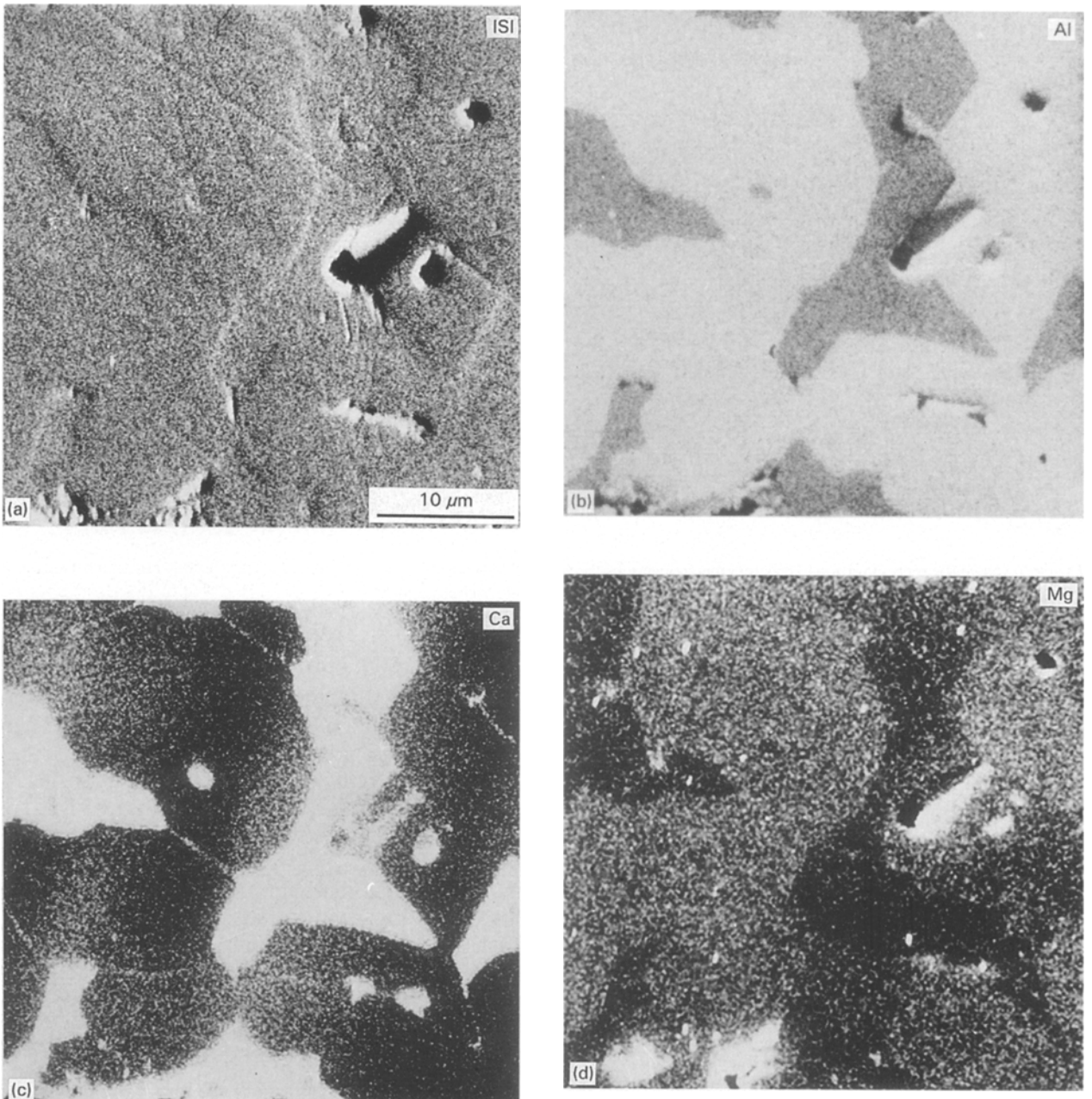

Figure 5 Corresponding SIMS images obtained from specimen A: $30CA_6$ (3): (a) ISI, (b) Al^+, (c) Ca^+, (d) Mg^+, and (e) Si^+. As for Figure 4, images are shown using a logarithmic gray scale to aid contrast interpretation. In contrast to the platelet composite, in this sample the magnesium concentration is higher in the alumina matrix than in the equiaxed CA_6 grains.

formation was 1100 °C. Accordingly, the hexaluminate must be formed by further reaction between CA and alumina, which can occur by two distinct mechanisms (see Fig. 6). One possibility is that the CA_6 nucleates at the interfaces between alumina and CA particles, and that the reaction proceeds by solid state diffusion through the reactant phase. However, if the surfaces of the CA and alumina grains are already wet by a liquid phase, the transformation to CA_6 would by necessity take place via a solution precipitation reaction. It is proposed, therefore, that reaction by solid state diffusion results in the formation of equiaxed CA_6 grains, whereas solution precipitation favours the development of platelet grains.

As for the nature of the aforementioned liquid phase, it is believed that the anorthite does not play

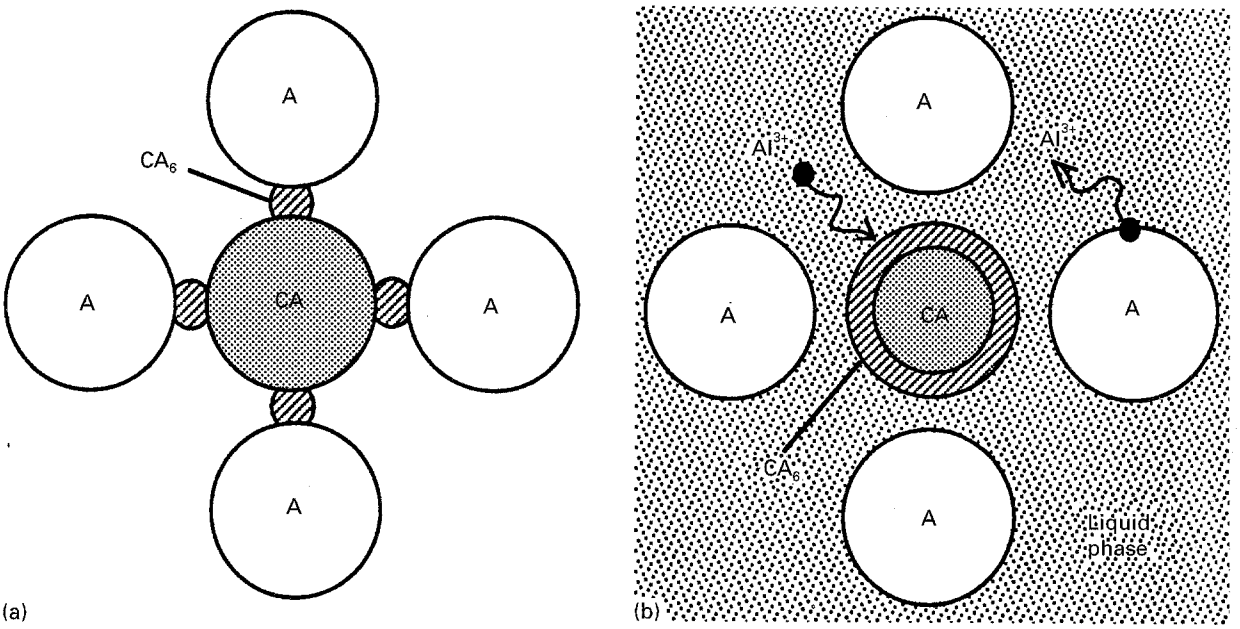

Figure 6 Schematic representation of different mechanisms for the reaction of CA and Al_2O_3 to form CA_6: (a) Solid state reaction between CA and Al_2O_3 grains, (b) solution-precipitation.

a significant role in the early stages of microstructure development, since previous work by Hummel and Arndt [18] has shown that on heating, crystallization of anorthite glass begins at 950 °C, and that below this temperature, the viscosity (>9.2 Poises) is too high for any appreciable flow. Moreover, with continued heating, the viscosity does not decrease significantly until the melting point of crystalline anorthite is exceeded (1550 °C). Instead, it is postulated that localized melting takes place as a result of a low temperature eutectic reaction in the $CaO–Al_2O_3$ system ($T_{eut} \sim 1390$ °C) [10], and it is this eutectic liquid which plays the dominant role in affecting the CA_6 reaction mechanism. This assertion is bourne out by Fig. 1, which shows that sample 1 (which contained 1 vol % anorthite) exhibited the identical microstructure development behaviour to sample 2 (no anorthite).

It has been postulated that the difference in the final microstuctures lies in the extent to which solid state reaction has occurred between CA and alumina, *prior to wetting by the liquid phase*. Clearly this will depend on a complex variety of factors including particle size, packing density, and how uniformly the $CaO/CaCO_3$ and Al_2O_3 powders are dispersed. Nonetheless, it is believed that all other considerations being equal, due to its higher reactivity, CaO will react more rapidly to form CA and subsequently CA_6. One could argue that since the carbonate phase will decompose to form the oxide at relatively low temperatures, any differences in the progression of the reaction would be minor. However, it should be noted that although the nominal decomposition temperature of $CaCO_3$ is 900 °C, in a pressed compact build up of CO_2 partial pressure could occur, so that the carbonate phase would be retained to higher temperatures. Furthermore, even slight differences in the degree of connectivity between CA and alumina particles could have an appreciable effect on the subsequent wetting behaviour and microstructure development.

4.3. Influence of magnesium

As mentioned previously in Section 2, chemical analysis of the $CaCO_3$ and CaO starting powders revealed that the overall concentration of Mg^{2+} was almost identical in both cases (< 10 ppm). The difference in the distribution of magnesium (as revealed by the SIMS maps of the sintered microstructures) is puzzling, and somewhat difficult to rationalize. One possibility is that it is a consequence of the different CA_6 reaction mechanisms. Since the matrix concentration of Mg^{2+} is higher in the equiaxed composite, the implication is that there is greater mobility of magnesium through the composite microstructure via solid state diffusion, than by diffusion through the intergranular liquid phase.

On a final note, the beneficial effect of small additions of MgO in preventing abnormal grain growth in alumina is well-documented [19, 20]. To test whether it would have the same effect in the present system, a sample having the same starting composition as A: CA_6 (1) was prepared, but with the deliberate addition of 100 ppm MgO. Interestingly, the aspect ratio of the CA_6 grains was markedly reduced! This result demonstrates unambiguously that the Mg concentration level can influence the CA_6 grain morphology in alumina:calcium hexaluminate composites. Since the Mg impurity level in the original A: $30CA_6$ (1) and A: $30CA_6$ (2) starting powders was insufficient to suppress anisotropic grain growth, it would appear that a critical concentration of Mg is required. In $LaAl_{11}O_{18}$, Chen and Chen [9] reported that 0.1 wt % Mg did not suppress the formation of elongated grains, except in the cases where other co-dopants (Mn, Li, Li and Si, Na and Si) were also added. Clearly the situation is a complex one, and detailed discussion of the precise mechanism is beyond the scope of this paper. Nonetheless, it is feasible that Mg promotes equiaxed grain growth in CA_6 in the same manner as it does in alumina, namely by reducing grain boundary mobility in boundaries not wet by liquid phase [21].

5. Summary

Reaction sintering between alumina and either a) $CaCO_3$ or b) CaO powders resulted in composites consisting of two-phase mixtures of alumina and calcium hexaluminate (CA_6). It was found that the morphology of the CA_6 grains depended on the precursor Ca containing powder. The use of $CaCO_3$ as the starting powder resulted in elongated platelet CA_6 grains, whereas CaO gave rise to equiaxed CA_6 grains. This result could not be satisfactorily attributed to differences in overall impurity concentration between the precursor powders. Instead, it is postulated that the difference in CA_6 morphology arises from differences in the reaction mechanism. In the case of CaO containing starting powders, it is believed that the higher reactivity of the CaO promotes a greater extent of solid state reaction between alumina and monocalcium aluminate, hence favouring the formation of equiaxed CA_6 grains. Conversely, platelet CA_6 is formed via a solution precipitation reaction, which predominates when extensive prior wetting of the parent phases has taken place.

Acknowledgements

The authors would like to thank A. G. Adriaens for performing the SIMS analysis, and Drs B. R. Lawn, M. P. Harmer and A. M. Thompson for taking part in many stimulating discussions concerning the work. The financial support of AFOSR (contract # F49620–92–J–0039, monitored by Dr A. Pechenik) is also gratefully acknowledged. One of the authors (KKS) would also like to acknowledge the support of NSF through the MRSEC at the University of Chicago.

References

1. C.-W. LI and J. YAMANIS, *Ceram. Eng. Sci. Proc.* **10** (1989) 632.
2. J. A. SALEM, S. R. CHOI, M. R. FREEDMAN and M. G. JENKINS, *J. Mater. Sci.* **27** (1992) 4421.
3. C. -W. LI, D. -J. LEE and S.-C. LUI, *J. Amer. Ceram. Soc.* **75** (1992) 1777.
4. S. R. CHOI, J. A. SALEM and W. A. SANDERS, *ibid.* **75** (1992) 1508.
5. N. HIROSAKI, Y. AKIMUNE and M. MITOMO, *ibid.* **76** (1993) 1892.
6. K. TSUKUMA and T. TAKAHATA, *Mater. Res. Soc. Symp. Proc.* **78** (1987) 123.
7. R. A. CUTLER, R. J. MAYHEW, K. M. PRETTYMAN and A. V. VIRKAR, *J. Amer. Ceram. Soc.* **74** (1991) 179.
8. J.-F. TSAI, U. CHON, N. RAMACHANDRAN and D. K. SHETTY, *ibid.* **75** (1992) 1229.
9. P.-L. CHEN and I.-W. CHEN, *ibid.* **75** (1992) 2610.
10. "Phase Diagrams for Ceramists, Vol. IV", R. S. ROTH, T. NEGAS and L. P. COOK, *Amer. Ceram. Soc.*, Columbus, OH, 1981.
11. A. UTSUNOMIYA, K. TANAKA, H. MORIKAWA, F. MARUMO and H. KOJIMA, *J. Sol. State Chem.* **75** (1988) 197.
12. E. CRIADO, P. PENA and A. CABALLERO, in Science of Ceramics 14, edited by D. Taylor, Inst. of Ceramics, Shelton, Staffs. (1988) 193–198.
13. T. NAGAOKA, S. KANZAKI and Y. YAMAOKA, *J. Mater. Sci. Lett.* **9** (1990) 219.
14. D. BROOKSBANK, *J. Iron and Steel Inst.* **208** (1970) 495.
15. J. L. MENDOZA, A. FREESE and R. E. MOORE, Int. Forum on Advances in Refractories Technologies, 294–311 (1989).
16. R. LEVI-SETTI, J. M. CHABALA, K. L. GAVRILOV, R. MOGILEVSKY and K. K. SONI, *Scanning Microscopy* **7** (1994) 1161.
17. K. K. SONI, J. M. CHABALA, R. MOGILEVSKY, R. LEVI-SETTI, W. S. WOLBACH, K. ZHANG and S. R. BRYAN, *Surface and Interface Analysis* **21** (1994) 117.
18. W. HUMMEL and J. ARNDT, *Contrib. Mineral Petrol.* **90** (1985) 83.
19. R. L. COBLE, *J. Appl. Phys.* **32** (1961) 793.
20. S. J. BENNISON and M. P. HARMER, in *Ceramic Trans.* Vol. 7, Amer. Ceram. Soc., Westerville, OH, 1990, pp. 13–49.
21. C. A. BATEMAN, S. J. BENNISON and M. P. HARMER, *J. Amer. Ceram. Soc.* **72** (1989) 1241.

Received 4 April
and accepted 1 December 1995